THEORY OF THE GALVANOMAGNETIC PROPERTIES OF GRAPHITE - CONSEQUENCES OF TRIGONAL WARPING OF THE CONSTANT ENERGY SURFACES*

R.O. Dillon** and I.L. Spain, Dept.of Chemical Engineering, University of Maryland, University Park, MD 20740

The out-of-plane electronic overlap parameter, γ_3, appearing in the band theory of Slonczewski and Weiss, introduces many complexities into the electronic structure of graphite. The most striking effect is that the constant energy surfaces become warped with three-fold symmetry about the vertical edges of the Brillouin zone. Using a simplified model of the energy surfaces and taking $\gamma_3 = 0.29$ eV, the effect of this trigonal warping on the conductivity tensor components σ_{xx} and σ_{xy} was calculated(1,2). Based on this calculation, the present paper discusses the effect of trigonal warping on: 1.) the field dependence of the low temperature Hall coefficient, 2.) low field conductivity data and carrier densities derived from such data, 3.) carrier densities derived from an integral of σ_{xx} over the field, and 4.) the pressure dependence of the basal conductivity of graphite.

Hall Coefficient

Warping of an energy suface can exert strong effects on the Hall coefficient at weak and intermediate fields. At strong fields warping never affects the Hall coefficient and it asymptotes to the value of $R_\infty = 1/(P-N)e$. For graphite, the model results indicate that trigonal warping will have only a small effect on the Hall coefficient at weak fields. However, it can have a large effect at intermediate fields tending to make the Hall coefficient become positive (for the model calculation, the intermediate field range is $.02 \lesssim \omega\tau \lesssim 2$). This positive-going tendency may cause a sign reversal at intermediate fields. The reason this tendency occurs is that portions of negative curvature on the cross section in Figure 1 become important in determining the Hall coefficient.

A tendency for the Hall coefficient to become positive at intermediate fields is, in fact, observed at 4K and 77K as illustrated in Figure 2. At 298K thermal broadening reduces the effect of trigonal warping. Previous workers have tried to explain the field dependencies shown in Figure 2 in terms of mobile minority carriers dominating the weak-field behavior. However, the following difficulties arise with this interpretation: 1.) the graphite band model predicts the existance of minority holes , but the weak-field data in Figure 2 cannot be explained without both minority electrons and holes 2.) the switch from a minority electron to a minority hole at 77K as the specimen is changed from pyrolytic to natural graphite cannot be explained and 3.) the pressure dependence of the weak-field Hall coefficient predicts extremal area changes of the minority pocket which are quite different than the pressure dependence of minority carrier de Haas Van Alphen oscillations.

A consistent explanation of the data in Figure 2 is reached if the positive excursions at intermediate fields are interpreted in terms of trigonal warping. The weak field behaviors are explained in terms majority carriers, and the change between pyrolytic and natural graphite at 77K is explained by differences in scattering mechanisms.

*This research was supported by the Atomic Energy Commission.

**Now at Dept. of Material Science, 6532 Boelter Hall, University of California, L.A.,CA 90024

Low Field Conductivity

The trigonal warping modulates the velocity of carriers on the Fermi surface, such that their average velocity increases. This causes a conductivity enhancement as represented by the factor $\bar{\beta}$ in,

$$\sigma = (N+P)e\bar{\mu}\bar{\beta}(\gamma_3,B) \qquad (1)$$

where N and P are carrier densities, $\bar{\mu}$ is an average mobility without trigonal warping, and the average on β denotes a Fermi surface average. As illustrated in Figure 3 for the part of the model calculation dealing with the electrons, $\bar{\beta}$ is large at weak fields and then asymptotes to a strong field limit somewhat greater than unity. The model uses non-warped hole cross sections and thus minimizes the enhancement of σ_{xx} due to warping of the hole Fermi surface. Even so the model yields a 60% enhancement of $\sigma_{xx}(o)$, indicating that trigonal warping strongly influences the weak field conductivity behavior. Figure 4 shows the observed behavior using the slope, n, of a log-log plot of $[\sigma_{xx}(o)/\sigma_{xx}(B)] -1$ versus $\bar{\mu}B$. The anomoulous weak field behavior has previously been interpreted in terms of mobile minority carriers. However, the estimated density of minority carriers is too low for them to be strongly affecting σ_{xx}.

Figure 4 also shows the prediction of the model calculation. Although the magnitudes are different, this shows that trigonal warping can produce a minimum in n at the same field region as the observed minimum.

The effect of warping on σ_{xx} at low fields indicates that use of equation

$$N + P = \sigma_{xx}(o)/e\bar{\mu} \qquad (2)$$

to calculate carrier densities will result in error. Trigonal warping tends to increase both $\sigma_{xx}(o)$ and $\bar{\mu}$. Since these increases oppose each other in calculating N+P, the net result is very sensitive to the exact form of the warping. The model calculation yielded an over-estimation of N+P on the order of 10%. The major effect of warping in using equation (2) is then not this error, but the variation on n at weak fields shown in Figure 4. This variation of n makes it impossible to define $\bar{\mu}$ without arbitrariness(3).

Carrier Densities Based on Field Integrals

An alternative to equation (2) which has been used to derive carrier densities is based on

$$N + P = \frac{2}{\pi e}\int_0^\infty \sigma_{xx} dB \qquad (3)$$

The enhancement of σ_{xx} caused by warping indicates that N+P will be overestimated with this formula. The model calculation yields an overestimation of 22%. However, a more serious problem associated with the application of (3) is that σ_{xx} does not asymptote to a B^{-2} dependence at high fields as required in derivation of (3). Evidence of this problem is indicated in Fig. 4 where at $\bar{\mu}B = 8$, $n = 1.6$ instead of a value near 2. Figure 4 also indicates that this high field behavior is not caused by trigonal warping. At higher fields σ_{xx} asymptotes to approximately a B^{-1} dependence. Because of this, equation (3) cannot presently be meaningfully applied to graphite.

Pressure Dependence of Conductivity

Equation (1) shows that trigonal warping introduces a term $(d\ell n\bar{\beta}/d\ell n\gamma_3)(d\ell n\gamma_3/dp)$ in the logarithmic derivative of the conductivity with pressure. The calculation of this term is difficult because both β and $d\ell n\beta/d\ell n\gamma_3$ vary along the vertical edge of the Brillouin zone. The model calculations show that $d\ell n\bar{\beta}/d\ell n\gamma_3 \gtrsim 1$. This result indicates that the variation of conductivity with pressure cannot be satisfactorily interpreted without the β term because $d\ell n\bar{\beta}/dp$ is on the order of $d\ell nN/dp$.

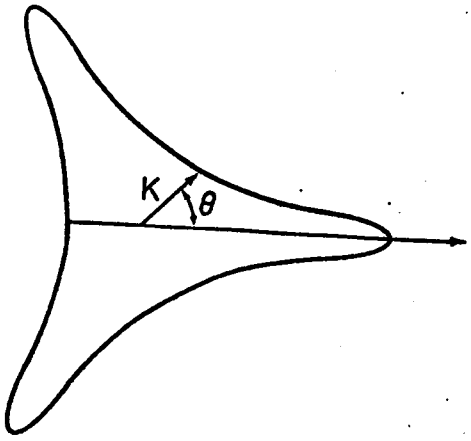

Figure 1. Cross section of the electron Fermi surface, based on $\gamma_3 = 0.29$ eV. The vector $\vec{K}$ points to a region of negative curvature.

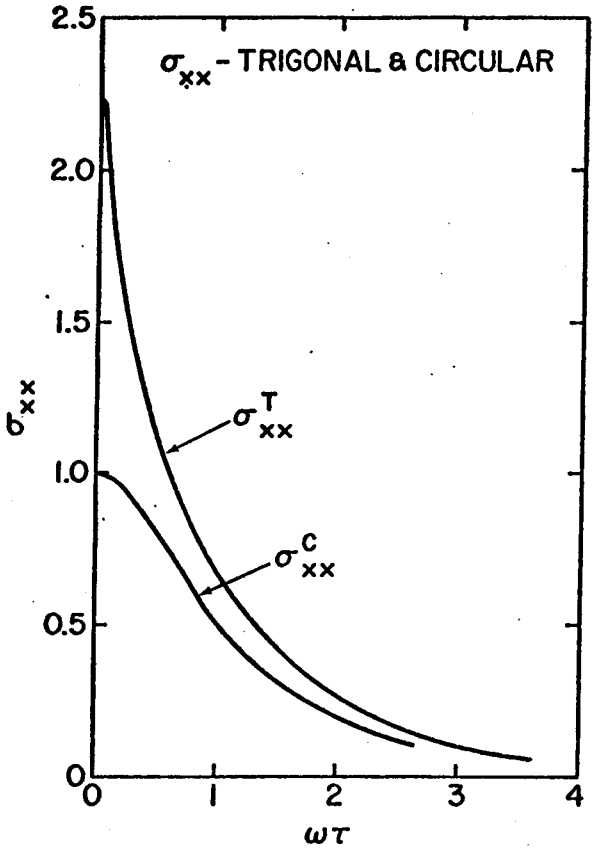

Figure 3. The normalized conductivity for the electron Fermi surfaces for circular, σ_{xx}^C, and trigonally warped, σ_{xx}^T, energy surfaces.

References

1. Dillon, R.O., Ph.D Thesis, University of Maryland (1974).
2. Dillon, R.O. and Spain, I.L., J.Phys.Chem.Solids, in press.
3. Spain, I.L. and Dillon, R.O., Carbon 14, p.23, (1976).

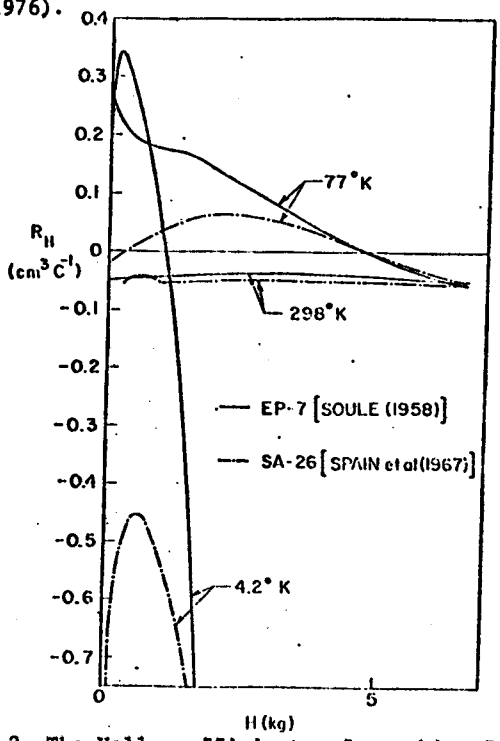

Figure 2. The Hall coefficients of graphite for pyrolytic (-·-) and natural (-) specimens.

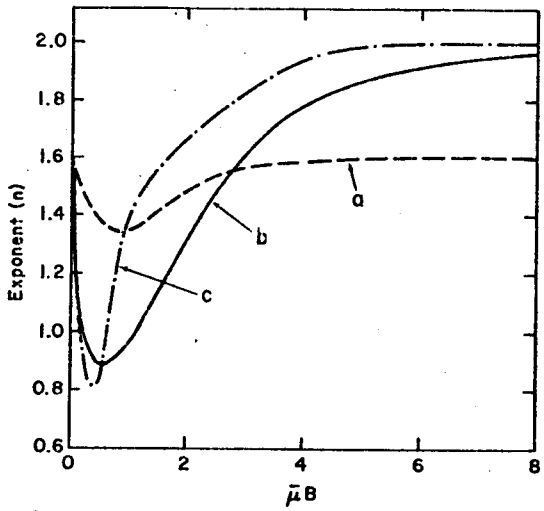

Figure 4. Variation of the slope, n, of a log-log plot of $[\sigma_{xx}(o)/\sigma_{xx}(B)] - 1$ versus $\bar{\mu}B$. Curves are for experimental data for pyrolytic graphite at 4.2K (a), and model calculation results, electron surface only (b) and both surfaces (c).